Journal of Engineering and Applied Sciences 13 (1): 105-118, 2018
ISSN: 1816-949X

Ozone Production Based on Photovoltaic Source

Waluyo, Deri Muhamad Nurendi, Syahrial and Nasrun Hariyanto
Department of Electrical Engineering, Institut Teknologi Nasional Bandung (ITENAS),
Jalan PHH Mustafa No. 23, 40124 Bandung, Indonesia

Abstract: Ozone has been studied for various applications. Nevertheless, it is still rare that involves photovoltaic source. The research was to make designing, implementing, wave form measuring and testing the ozone generation based on solar power generation with dc-dc converter. The corona discharge current waveforms were investigated due to dc voltages. The relations among the oxygen flows, voltage levels and oxygen debits to the ozone product were also investigated. Both voltage and discharge current waveforms were measured by using a storage oscilloscope and transferred to a computer. The discharge currents were occurred in around every 72.6 μsec intermittently. It was flowed 3 and 5 L/min of oxygen. It was yielded the greatest produced ozone in the third stage of voltage, 7.047 V, 5 L/min of oxygen debit and at minute of 50 that was 0.0323 mgO_3/L.

Key words: Corona, dc-dc power conversion, oxygen, ozone, solar power generation, generation

INTRODUCTION

Ozone has been currently studied for various applications such as water treatment, domestic and industrial effluent treatment, medicine dentistry, veterinary medicine, agriculture, disinfectant of environment and food preservation. An improvement in its generation by ozone generator system is fundamental. Ozone can be produced in three ways: by electrolysis, Ultra Violet (UV) and corona effect (Schiavon *et al*., 2012). Ozone is the triatomic state of oxygen that is a molecule comprising of three oxygen atoms. It is a relatively unstable and reactive gas (Smith, 2016).

Ozone is one of the most powerful chemical oxidizers and has many applications in industry. However, its use in industry as an oxidizing agent has been limited by the relatively low conversion efficiency of the ozone generator (Izeki, 1983). Despite, the small amount of generated ozone, there is enough to cause a variety of interesting oxidations (Mattson *et al*., 2007).

Ozone is negative impacts, such as strongly contributes to aging on polymeric and silicone rubber materials (Ma *et al*., 2010, 2011). Nevertheless, the ozone or corona discharge has positive impact, mainly for precipitation by Mizuno (2000) and Castle *et al.* (1969). Ozone is a by-product of corona discharge. Corona is observed in any forms including glows and haloes, spots, brushes and streamers. The potential at which corona is found to originate is called corona threshold voltage. Above this voltage, there is a limited region in which current increases proportionately with voltage called the Ohm's law regime. After this region, the current increases more rapidly, leading to the complete breakdown and arcing or sparking at a point called the breakdown potential. Corona discharge is highly dependant on geometry. Electric field intensity is higher around a surface of charged conductor with higher curvature or lower radii of curvature. When the electric field increases, it influences the atomic orbital and may cause atoms or molecules to polarize or liberate electrons. The maximum electric field that a dielectric material can withstand without conduction is known as a dielectric strength (Panicker *et al*., 2003; Loeb, 1965).

Ozone is manufactured in the corona discharge by drawing in air which is composed of 20% oxygen. This causes the oxygen molecules to dissociate and reassemble as ozone (LLC., 2015). The streamer type coronas used for ozone generation, generally use air or oxygen filled short gaps where one of the electrodes is covered with an insulating layer in order to prevent streamer-arc transition (Goldman *et al*., 1985). Electrically, ozone can be generated by breaking the oxygen molecules in a dielectric barrier discharge chamber. The important property of the dielectric barrier discharge is the creation of cold non-equilibrium plasma at atmospheric pressure condition. In the chamber, a high voltage is applied between two electrodes, one of which is covered with dielectric. Oxygen is forced to flow in a space between the electrodes, called discharge gap. If the electric field is sufficiently high, it breaks the oxygen molecules into its atoms, the latter then combines with other oxygen molecules to ozone form. Excessive concentrations of

Corresponding Author: Waluyo, Department of Electrical Engineering, Institut Teknologi Nasional Bandung (ITENAS), Jalan PHH Mustafa No. 23, 40124 Bandung, Indonesia

ozone at the ground level have adverse respiratory effects in humans (Ketkaew, 2007; Seinfeld and Pandis, 1998).

Some characteristics, modeling, effects and harmonics on ozone or corona discharge have been investigated (Patil and Vijayan, 2010; Szczepanski *et al*., 2017; Pontiga *et al*., 2001; Ohkubo *et al*., 1990; Boonseng *et al*., 2000). Gaseous ozone is toxic, e.g., the OSHA permissible exposure limit in air is only 0.1 ppm for an 8 h exposure. This concentration can be achieved by aqueous ozone concentrations of 0.018 ppm in pools and 0.011 ppm in spas. The limit for as shorter exposure, 10 min is 0.2 ppm (Wojtowicz, 2001). Ozone is used in industry as an oxidizing agent has been limited by the relatively low conversion efficiency of the ozone generator. For example, typical commercial ozone generators utilize about 5% of the input power in ozone production (Izeki, 1983). The temperature could influence the productivity of ozone. The relationship of temperature and ozone generating efficiency could be shown in mathematic polynomial equation (Sathalalai and Khan-ngern, 2009). It was be told the history of medical ozone and its other applications (Pressman, 2001).

The electric field intensity could be used as a type of ozone generator (Charlangsut *et al*., 2010). The generated ozone concentration was very dependent upon the value of pulse forming capacitance and ozone generator capacitance and corona tip-to-tip distance of the discharge electrode (Moon, 1992). Ozone could be generated or produced by various methods such as DC, pulsed and negative wire-to-cylinder corona discharges (Pontiga *et al*., 2007; Chalmers *et al*., 1996; Yanallah *et al*., 2008), gas discharge (Samaranayake *et al*., 2001), streamer corona (Fukawa *et al*., 2008; Vijayan and Patil, 2011) and high frequency (Udhayakumar *et al*., 2016). Another proposed of ozone generator using a phase-shift PWM full bridge inverter as a power supply. It offering high voltage and high frequency is capable of generating ozone (Hothongkham and Kinnares, 2009). A high frequency plasma generator experimental model was designed and built to study the behavior of the corona discharge at MHz frequencies and using inverter (Tudoran, 2011; Tsai and Ke, 2009). The L-C resonant circuit-based power supply used in ozone generation has been also investigated without a transformer (Amjad *et al*., 2012, 2013). A plasma generator composed of high frequency, high voltage transformer, discharging electrodes and zero voltage switching resonant converter has been proposed with their associated equivalent circuits (Yong-Nong and Chih-Ming, 2013).

Ozone concentration measurements have been evaluated to the ozone production, yield and production energy cost. The ozone production yield and cost vary in the range of 15-55 g/kWh and 35-110 eV/molecule (Simek and Clupek, 2002). The maximum ozone generation concentration and ozone generation efficiency are obtained with the meshed-plate type electrode (Park *et al*., 2006) and the highest energy efficiency for ozone production was obtained using high voltage pulses of approximately 150 n sec duration in Ar/O_2 mixtures (Lukes *et al*., 2005).

In other hand, the solar energy source potential is 4.8 $kWh/m^2/day$ in Indonesia (Anonymous, 2016). A prototype system of ozone generator using solar energy could generate ozone gas from air at approximately 20 mgO_3/h (Potivejkul *et al*., 1998). Based on, the above literatures, it was necessary to make design, implementation and test a ozone generator based on photovoltaic source.

The objectives of research were to make design, implementation, measurements and tests the ozone generator based on a photovoltaic source with flyback converter. It was investigated the corona discharge current waveforms due to dc voltages. The relations among the oxygen flow time, 10-50 min in 10 min steps, voltage levels and oxygen debits to the product of ozone concentrations were also investigated. As a comparison, it was investigated the corona discharge current waveforms based on the back up battery source.

MATERIALS AND METHODS

Figure 1 shows the basic planning block diagram of photovoltaic based ozone generation. The photovoltaic

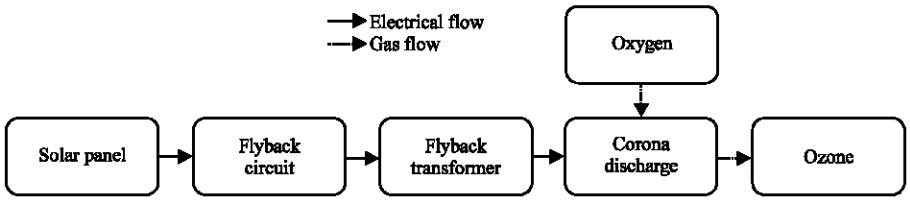

Fig. 1: Block diagram of photovoltaic based ozone generation

panel would produce the voltage of 12 V_{dc} nominally, it could reach 18 V_{dc}. Furthermore, this voltage would be raised to a high voltage which finally it was necessary to generate the ozone.

The specification of the used photovoltaic panel was 100 W_p of power. The open circuit voltage was 21.5 V, the short circuit current (I_{sc}) was 6.46 A, the Voltage at maximum power (V_{mp}) was 17.5 V_{dc} and the current at maximum power (I_{mp}) was 5.72 A. The flyback circuit, in Fig. 2, served to produce variable voltages (Nurendi *et al*., 2015). Here was a chopper circuit used in the design of the ozone generator.

Figure 2, it was used RC oscillator circuit as the oscillator generation. The used transistors in the circuit were made up of transistors TIP32C and BU4522AF. The function TIP32C PNP transistor was for an amplifier to a digital circuit. While BU4522AF transistor was as a trigger in the circuit that served to supply current to the transformer. BU4522AF transistor also served as a safety in the event of over current. The following equations are used to calculate the above circuit:

$$f = \frac{1}{T} \quad (1)$$

$$f_0 = \frac{1}{2\pi RC} \quad (2)$$

$$C = \frac{C_1 x C_2}{C_1 + C_2} \quad (3)$$

$$V_1 = \frac{R_3}{R_1 + R_2 + R_3} V_{in} \quad (4)$$

$$V_2 = \frac{R_8}{R_7 + R_8} V_1 \quad (5)$$

$$V_B = V_2 - V_{BE} \quad (6)$$

$$I_B = \frac{V_B}{R_9} \quad (7)$$

In this research, after obtaining the high voltage, it was necessary to produce ozone. The high voltage was connected to the plate conductor as generator of corona, taken place with 3 variables for each condition by adjusting the voltage to generate corona and two oxygen debits for ozone production. Figure 3 shows the planned electrodes that would generate ozone gas that insulated by Pyrex tube.

When the electric field at the surface of energized conductor exceeds 2-3 kV/mm, audible and sometimes visible corona discharges occurs (Jones, 1972). In this research, the Pyrex insulator tube was designed that had the following specification: 30 cm in length, 20 mm in diameter, 10 mm in radius and 0.5 mm in radius of inside copper conductor.

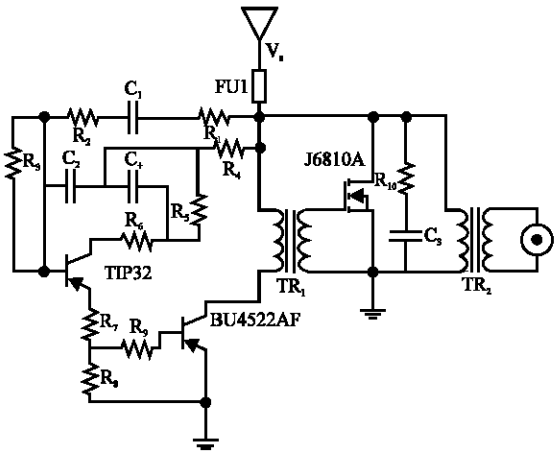

Fig. 2: Flyback circuit

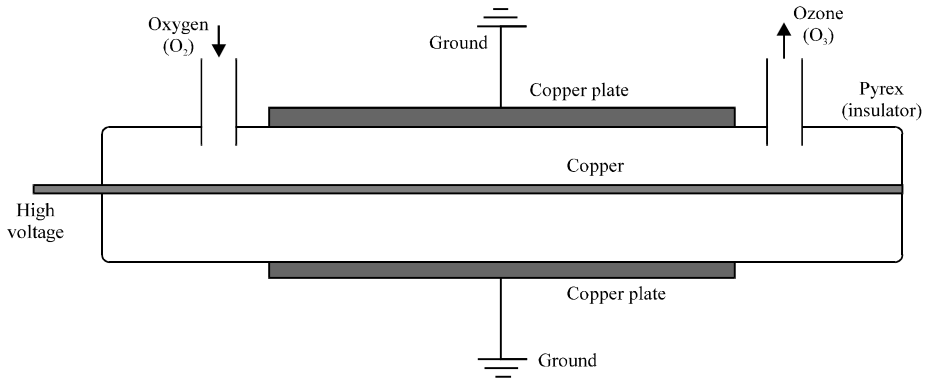

Fig. 3: Ozone generation electrodes

The used electrodes was installed in two different places, namely inside the tube and outside covering, circular, the Pyrex tube. Corona discharge begins when an electric field around the active electrode to form highly curved geometry has the ability to ionize the gas species (Moon and Jung, 2007). To determine the distance (x) that corona appeared, furthermore, the electric field in this experiment could be determined by the following Eq. 8:

$$E = \frac{V}{x \ln\left(\frac{R}{r}\right)} \quad (8)$$

Where, E, V, x, R and r were electric field, applied voltage, distance of the corona occurred, outside conductor radius on the cylinder and copper wire radius, respectively. The minimum voltage to be corona could be calculated using Eq. 8, namely for 2 kV/mm electric field. Thus, the necessary minimum voltage was 2.996 V or around 3 kV. Nevertheless, the generated voltage in the designed circuit was around 3-7 kV. Therefore, the maximum distance that corona discharge occurred was 1.3 mm radius.

In this testing, the voltage source from the photovoltaic source was raised by the flyback circuit, including the flyback transformer up to around 7 kV. Therefore, it would require a voltage divider circuit to facilitate the measurement up to around 7 kV. Thus, to get the original value of the measurement results, it should be carried out the following voltage divider circuit as Fig. 4 and the calculation method as Eq. 9:

$$V_i = \left[\frac{R_1 + R_2}{R_2}\right] V_0 \quad (9)$$

Where V_i and V_o were the real voltage and the voltage measurement reading result. The resistors of the voltage divider were R_1 = 5.6, X 19 = 106.4 and R_2 = 3.3 MΩ. Besides that, the differential probe multiplier constant was 500 times and the attenuation factor of the oscilloscope was 10. Thus, the multiplier factor of the recorded values in the storage digital oscilloscope to the real values was 1.662. Figure 5 shows the diagram of photovoltaic source ozone generation including the measuring system.

Photovoltaic power panel generated 12 up to 18 V_{dc} source. This dc source was connected to the flyback circuit of supply voltage. Having obtained the desired voltage, the voltage was raised by using the flyback transformer to generate corona. The oxygen in the gas tube was flowed into the reactor through the pipes at a rate that was set by the flow meter. The result of the oxygen flowing in the corona reactor tube was ozone. The generated ozone existence amount could be measured by using a spectrophotometer as an ozone monitor.

The measurement of remaining ozone concentrations in this experiment were actually the concentration of residual ozone. This case was due to the nature of ozone gas which was reactive. The ozone reactivity complicated for measurement of ozone solubility in water directly. To perform the calculation of the concentration of residual

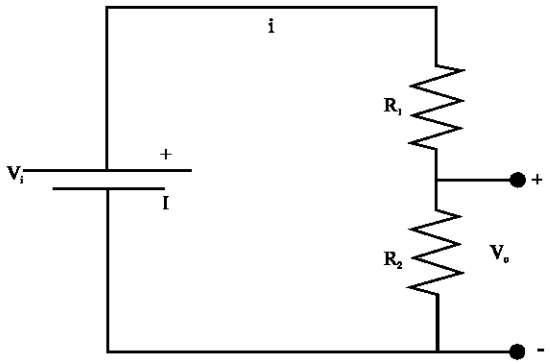

Fig. 4: Voltage divider circuit

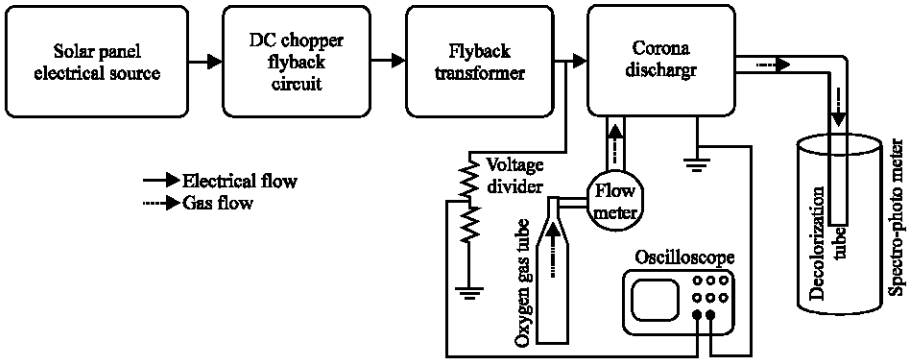

Fig. 5: Diagram of photovoltaic source ozone generation including the measuring system

ozone in the water, it was necessary to be done using the indigocalorimetry method and assisted by the spectrophotometer and by following Eq. 10:

$$C = \frac{50 \times \Delta A}{fxbxv}\left[\frac{mgO_3}{L}\right] \quad (10)$$

Where:

ΔA = The difference of Absorbance between samples and blanks
b = The length of the used cuvette (4.5 cm)
v = The volume of sample water (9 mL)
f = The 0.42 (based on the sensitivity factor of 20,000/cm for the change of absorbance 600 nm per mole of the addition of ozone per liter

RESULTS AND DISCUSSION

Figure 6 shows the main components of implemented photovoltaic source based ozone generation. Figure 6a is the panel that used as photovoltaic energy source. The used photovoltaic was 100 W_p as energy conversion from the sun light to the electric energy. Figure 6b shows the flyback dc chopper circuit and flyback transformer. The circuit generated high frequency as chopper of dc voltage. Furthermore, this dc voltage was multiplied to be high voltage by flyback transformer. The dc high voltage was entered to the electrode for producing corona discharge. Figure 6c shows the voltage divider for the measuring purpose of yielded high voltage to the storage digital oscilloscope. Finally, Figure 6d shows the ozone generator electrode where the device produced the ozone as consequence of corona discharge (Nurendi *et al*., 2015).

The instruments for corona measurements were a differential probe, digital storage oscilloscope and laptop or computer. The differential probe was for reducing the measured signals and safety purposes. The digital storage oscilloscope was as main instrument for applied high voltage and discharge current waveform measurements and the computer was for data savings after transferred from the digital storage oscilloscope. These data could be carried out for further analysis. Figure 7 shows the main instruments of oxygen and ozone measurements. Figure 7a shows oxygen tube which contained oxygen gas. The oxygen gas in this research was as raw material to produce ozone. Another one was a container tube to accommodate the generated ozone gas. Figure 7b shows a spectrophometer to measure the concentration of generated ozone gas.

In this testing, the voltage source of the photovoltaic was raised by the flyback circuit and flyback transformer up to around 7,000 V. Therefore, it would required a voltage divider circuit to facilitate the measurements. Thus, to obtained the original value of the measurement results, it should be carried out to be multiplied certain factors. The calculation results based on Eq. 1 until Eq. 7 were 7,692.4; 7,525 Hz; 23.5 nF; 7.73 V; 5.26; 4.56 V and 9.7 mA, respectively. The electric field could be determined by using Eq. 8. It could be generated from every stage voltage, using 0.5 and 10 mm for inside and outside copper conductor radius, respectively. The calculation results of electric field are listed in Table 1.

Based on the calculations results of electric field, it was corona occurred in the design ozone reactor tube, both from the photovoltaic and battery sources as a comparison. In the maximum conditions, the output high voltages based on the photovoltaic were lower than those based on the battery, although, the photovoltaic voltage output was higher, 18 V_{dc}, than the battery voltage, 12 V_{dc}.

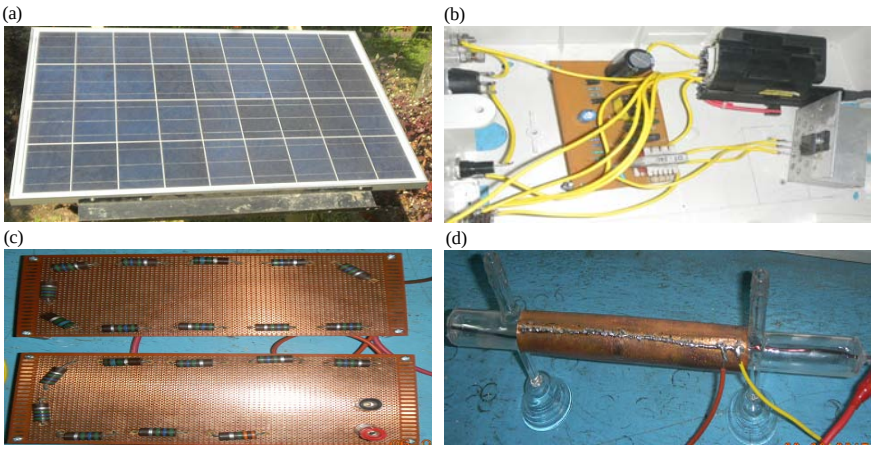

Fig. 6: The main components of photovoltaic based ozone generation: a) Solar panel; b) Flyback circuit and ignition coil; c) Voltage divider and d) Ozone generating electrode

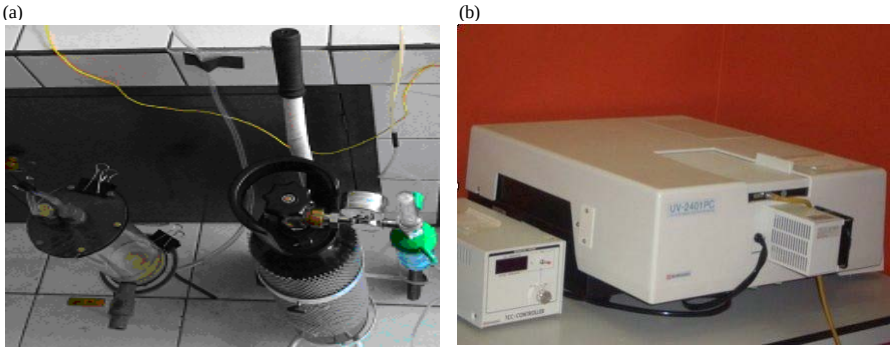

Fig. 7: The main instruments of oxygen and ozone measurements: a) Oxygen and ozone tubes and b) Spectrophometer

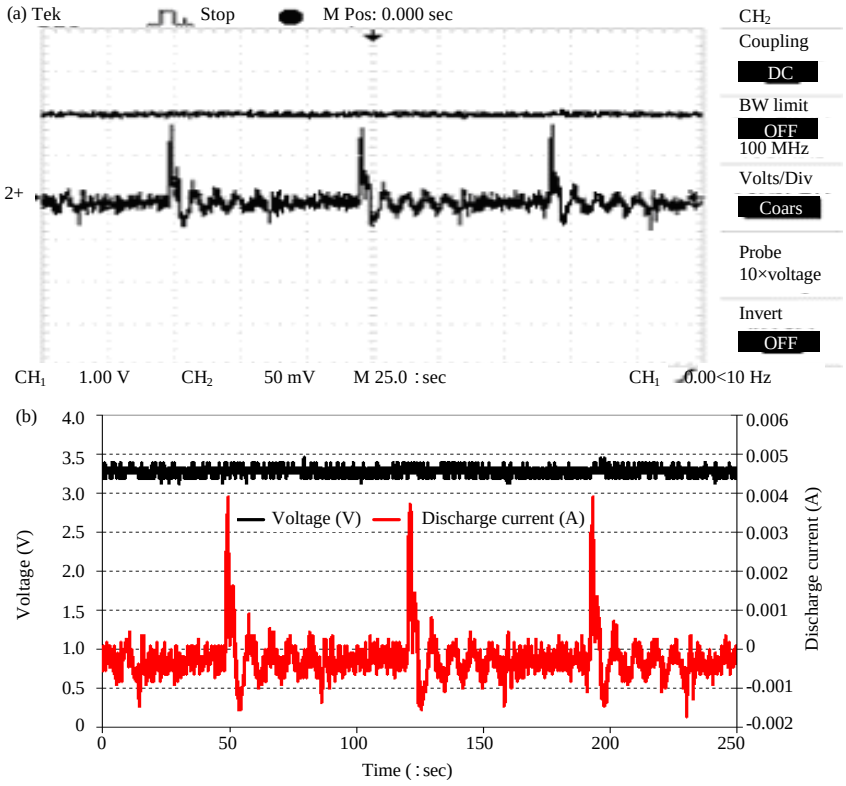

Fig. 8: The voltage and discharge current versus time on first stage: a) Original display and b) Converted display

Table 1: The calculations results of electric field

Stages of voltage	Photovoltaic output dc hv (V)	Photovoltaic output dc hv elelctric field (kV/cm)	12 V_{dc} battery output hv (V)	12 V_{dc} battery output dc hv elelctric field (kV/cm)
1	3.391	22.64	4.488	29.96
2	6.250	41.72	6.582	43.94
3	6.948	46.38	7.047	47.05

Thus, the electric field would be lower too. This case indicated that the battery was more stable due to corona discharge than the solar panel. Fig. 8 shows the voltage and discharge current versus time on first stage where Fig. 8a is the original bitmap display and Fig. 8b is excel converted display. In this stage, the source voltage V_s from the photovoltaic was 18 V_{dc}, the voltmeter reading for the output voltage V_o was 75 V_{dc} and the converted calculation voltage for the output voltage V_o was 3391 V_{dc}. It was also indicated that based on this voltage, the peak discharge current was 3.9 mA in intermittent that signed corona appearing in the reactor tube.

Figure 9 shows that in the second stage with the source voltage of 18 V_{dc} from the solar panel where Fig. 9a is the original bitmap display and Fig. 9b is excel

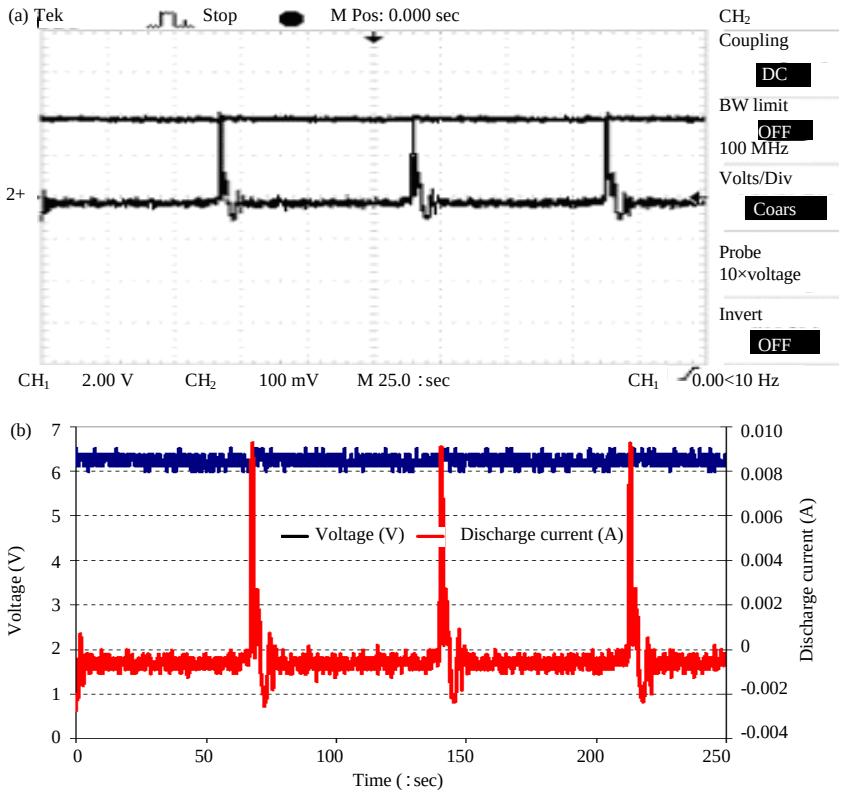

Fig. 9: The voltage and discharge current versus time on the second stage: a) Original display and b) Converted display

Table 2: The generated residual ozone concentration of the photovoltaic source first stage voltage

	3 l/min oxygen debit (Q)		5 l/min oxygen debit (Q)	
Time (min)	ΔA	mgO_3/L	ΔA	mgO_3/L
10	-0.005	-0.0147	-0.003	-0.0088
20	-0.003	-0.0088	-0.001	-0.0029
30	0.001	0.0029	0.001	0.0029
40	0.001	0.0029	0.003	0.0088
50	0.003	0.0088	0.004	0.0118

converted display. The voltmeter reading of output voltage was 180 V_{dc}. Thus, the output voltage became 6.250 V_{dc} that cause the peak discharge current of 9.2 mA in intermittent, indicating the appearance of the corona on the reactor tube.

Figure 10 shows that in the third stage with the source voltage of 18 V_{dc} from the solar panel where Fig. 10a is the original bitmap display and Fig. 10b is excel converted display. The voltmeter reading of output voltage was 200 V_{dc}. Thus, the output voltage became 6.948 V_{dc} that cause the peak discharge current of 11.2 mA in intermittent, indicating the appearance of the corona on the reactor tube.

Table 2 shows the number of absorbance measurement results using the spectrophotometer from the water sample that have undergone ozonation reaction with oxygen debit of 3 and 5L/min at the first

Table 3: Generated residual ozone concentration by the second stage voltage

	3 l/min oxygen debit (Q)		5 l/min oxygen debit (Q)	
Time (min)	ΔA	mgO_3/L	ΔA	mgO_3/L
10	-0.003	-0.0088	-0.001	-0.0029
20	-0.002	-0.0059	0.001	0.0029
30	0.001	0.0029	0.003	0.0088
40	0.003	0.0088	0.004	0.0118
50	0.005	0.0147	0.007	0.0206

voltage stage with 3.391 V_{dc} that has been raised by using the flyback circuit from the source of 18 V_{dc} output of solar panel. Table shows that each increment of interval time reveals the increase in the absorbance and the ozone concentration values of that have been produced.

Table 3 shows the number of absorbance measurement results using the spectrophotometer from the water sample that have undergone ozonation reaction with the oxygen debit of 3 and 5 L/min at the second stage from the photovoltaic source voltage of 18 V_{dc} where it was increased by using the flyback circuit upto 6.250 V_{dc}. Table shows that each increment of interval time reveals the increase in the absorbance and the ozone concentration values of that have been produced.

Table 4 shows the number of absorbance measurement results using the spectrophotometer from

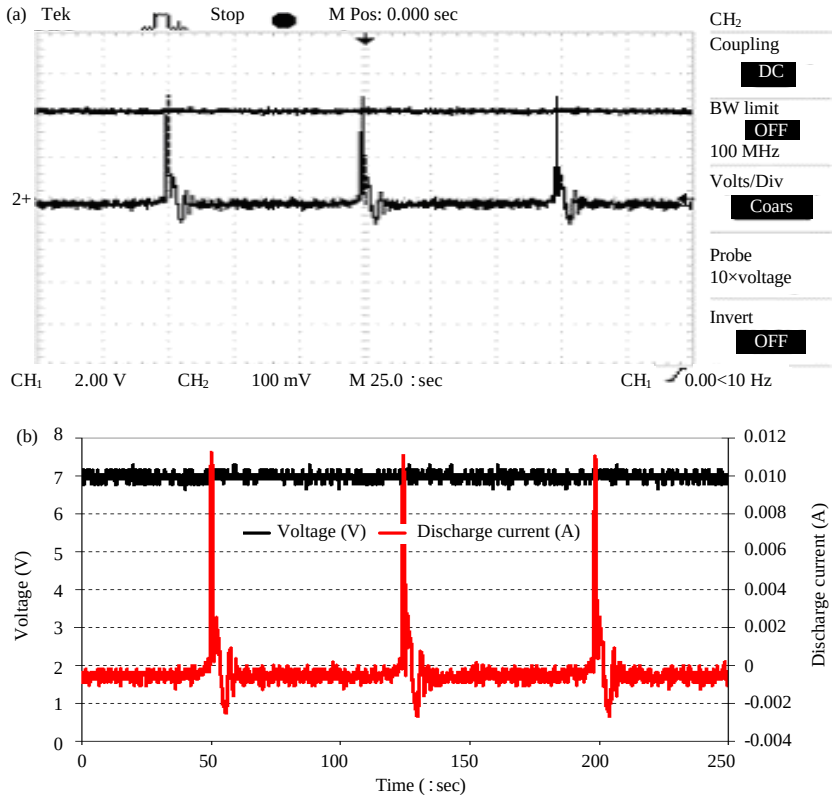

Fig. 10: The voltage and discharge current versus time on the third stage: a) Original display and b) Converted display

Table 4: Concentrations of residual ozone generated by the third stage voltage of photovoltaic source

	3 l/min oxygen debit (Q)		5 l/min oxygen debit (Q)	
Time (min)	ΔA	mgO_3/L	ΔA	mgO_3/L
10	-0.002	-0.0059	0.001	0.0029
20	0.002	0.0059	0.003	0.0088
30	0.003	0.0088	0.006	0.0176
40	0.005	0.0147	0.008	0.0235
50	0.008	0.0235	0.011	0.0323

water samples that have undergone ozonation reaction with the oxygen debit of 3 and 5 L/min at the third stage voltage of the photovoltaic source which has been raised using the flyback circuit from source 18 V_{dc} became 6.948 V_{dc}. Table 4 shows each increment of time reveals the increase in the absorbance and ozone concentration values that have been produced.

Figure 11 shows the relationship between the concentration of ozone and the ozonation time in the setting of oxygen flow rate of 3 and 5 L/min. These curves show the first, second and third stages of voltage. It reveals that the concentration of ozone product due to oxygen flow rate of 5 L/min would be higher than that 3 L/min. Besides that, the concentration of ozone product would rise as the voltage level increased and also the time increased too. The most substantial ozone formed

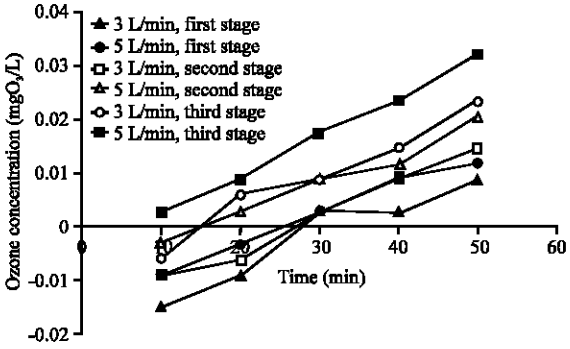

Fig. 11: Relationship between the ozonation time and the remaining ozone concentration in the oxygen debit of 3 and 5 L/min, for first, second and third stages of photovoltaic source

is shown in the stage 3 with the voltage of 6.948 V_{dc}, the oxygen flow rate of 5 L/min that produce ozone of 0.0323 mgO_3/L at 50 min.

Figure 12 shows a graph of the residual ozone concentration to voltage for 50 min. It can be seen that the formed ozone would increase as the voltage rise. It also reveals that the oxygen flow of 5 L/min would produced the ozone concentration greater than that the oxygen flow of 3 L/min.

As comparison, Fig. 13-15 show the voltage and discharge current versus time based on the 12 V_{dc} battery source (Nurendi *et al.*, 2015). Figure 14 shows the voltage and discharge current versus time for first stage. The voltmeter reading for V_o was 135 V_{dc} and the converted calculation voltage was 4.488 V_{dc}. It was also indicated that based on this voltage, the peak discharge current was 10.5 mA in intermittent that signed corona appearance in the reactor tube.

The data in Table 5 are the concentrations of residual ozone in water. The number of measurement results used the spectrophotometer absorbance of water sample had undergone the ozonation reaction with the oxygen debit of 3 and 5 L/min. Table also shows each increment of time that shows the increase of absorbing values.

Table 5: The generated residual ozone concentration of the battery source first stage voltage

	3 l/min oxygen debit (Q)		5 l/min oxygen debit (Q)	
Time (min)	ΔA	mgO_3/L	ΔA	mgO_3/L
10	-0.003	-0.0088	-0.004	-0.0118
20	0.002	-0.0059	0.002	-0.0059
30	0.003	0.0088	0.003	0.0088
40	0.004	0.0118	0.005	0.0147
50	0.006	0.0176	0.007	0.0206

Figure 14 shows that in the second stage, the output converted calculation voltage became 6,582 V_{dc} that cause the peak discharge current of 18.5 mA, indicating the appearance of the corona on the reactor tube. In this stage, the voltage meter reading V_o was 198 V_{dc}.

Table 6 shows the number of absorbance measurement results on the second stage voltage of 6582 V_{dc}. The table shows each increment of time reveals the increase in the absorbing values.

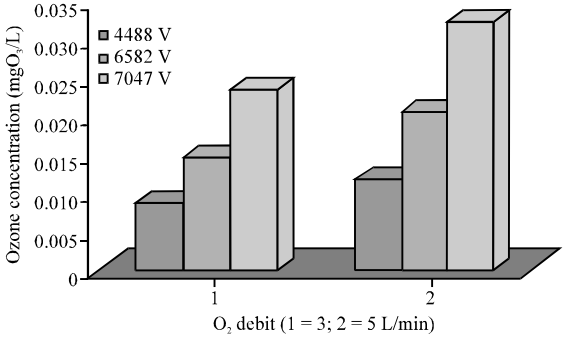

Fig. 12: The relationship between the remaining ozone concentration and voltage levels for both 3 and 5 L/min of oxygen debits in 50 min

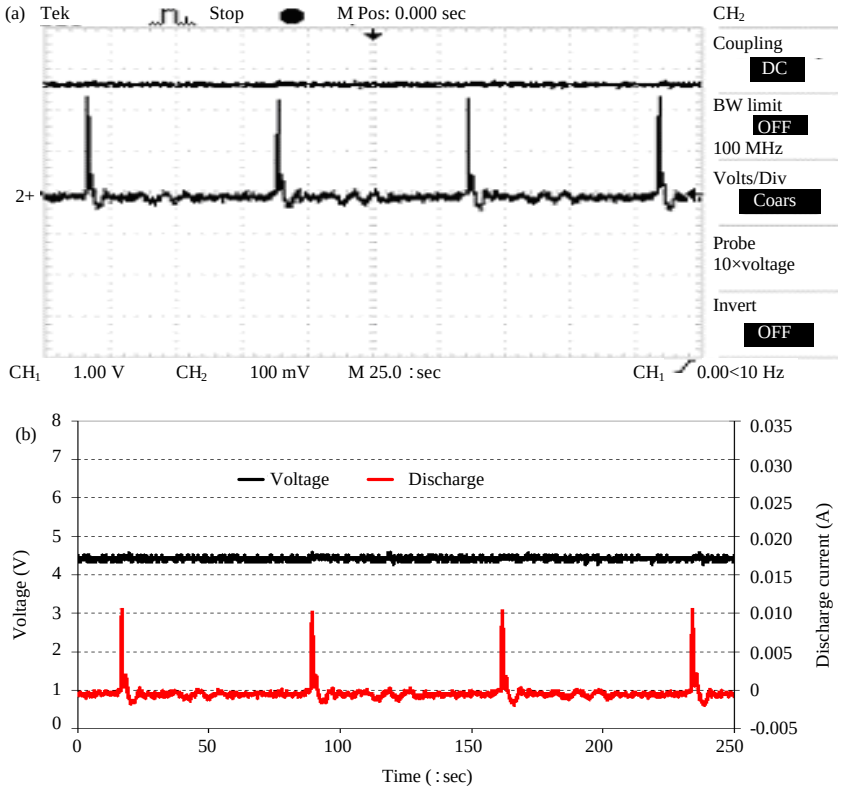

Fig. 13: The voltage and discharge current versus time on the first stage of battery source: a) Original display and b) Converted display

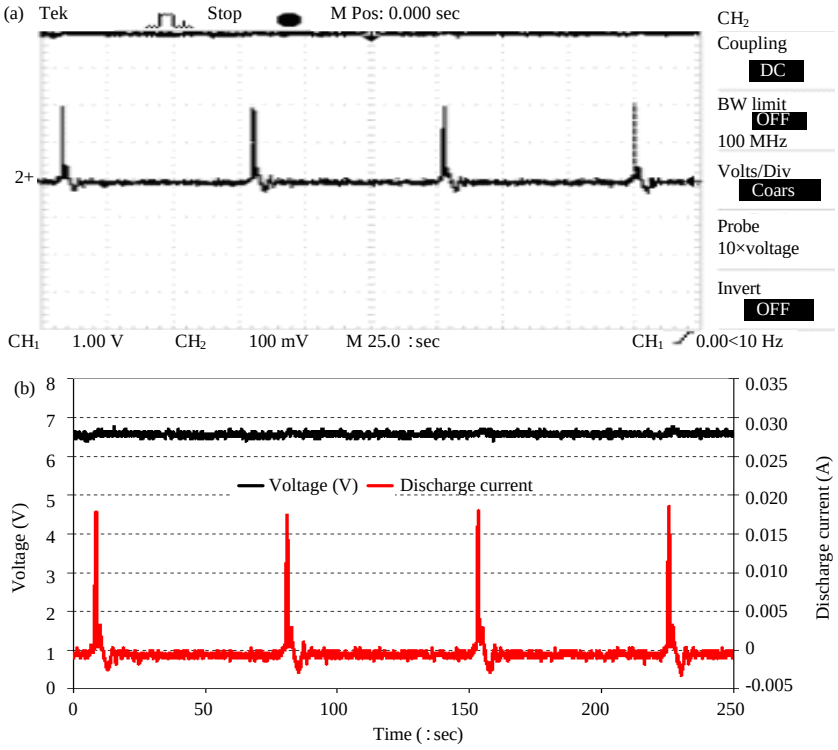

Fig. 14: The voltage and discharge current versus time on the second stage of battery source: a) Original display and b) Converted display

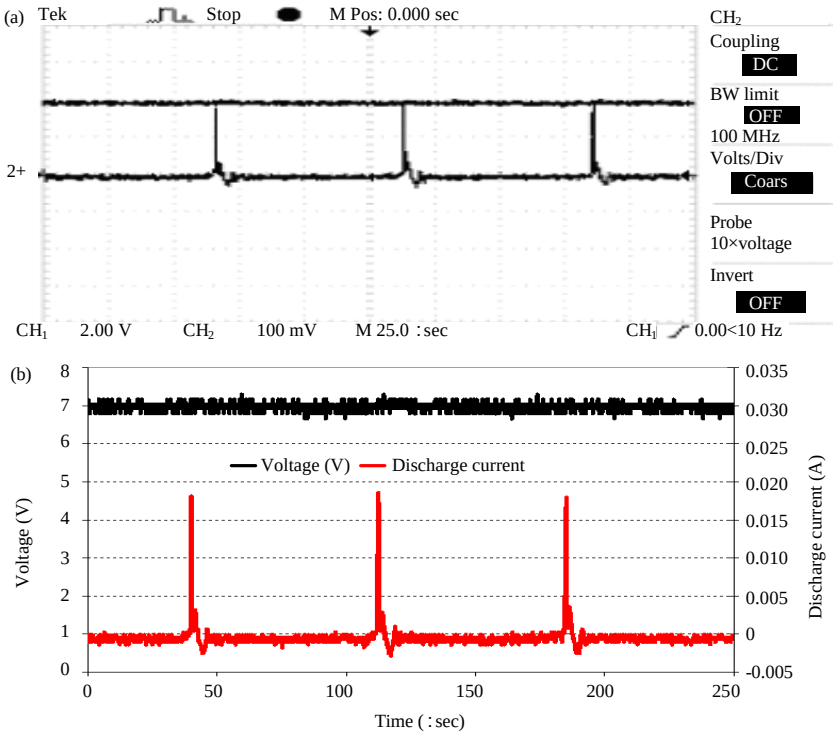

Fig. 15: The voltage and discharge current versus time on third stage of battery source: a) Original display and b) Converted display

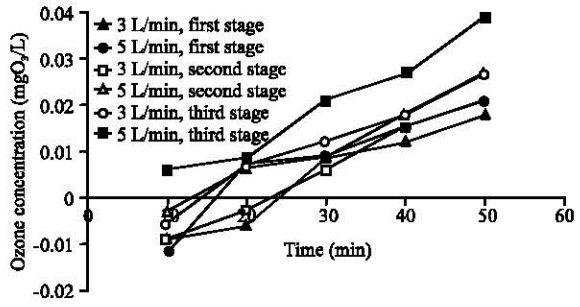

Fig. 16: Relationship between the ozonation time and the remaining ozone concentration in the oxygen debit of 3 and 5 L/min for first, second and third stages of battery source

Table 6: The generated residual ozone concentration of the battery source second stage voltage

	3 l/min oxygen debit (Q)		5 l/min oxygen debit (Q)	
Time (min)	ΔA	mgO_3/L	ΔA	mgO_3/L
10	-0.003	-0.0088	-0.001	-0.0029
20	-0.001	-0.0029	0.002	0.0059
30	0.002	0.0059	0.003	0.0088
40	0.005	0.0147	0.006	0.0176
50	0.007	0.0206	0.009	0.0265

Table 7: The generated residual ozone concentration of the battery source third stage voltage

	3 l/min oxygen debit (Q)		5 l/min oxygen debit (Q)	
Time (min)	ΔA	mgO_3/L	ΔA	mgO_3/L
10	-0.002	-0.0059	0.002	0.0059
20	0.002	0.0059	0.003	0.0088
30	0.004	0.0118	0.007	0.0206
40	0.006	0.0176	0.009	0.0265
50	0.009	0.0265	0.013	0.0382

Figure 15 shows that in the third stage, the output voltage was 7.047 V_{dc} which appearing the peak discharge current of 18.5 mA, indicating the appearance of corona on the reactor tube. The voltage reading was 212 V_{dc}.

Table 7 shows the number of absorbance measurement results using a spectrophotometer from water samples that have undergone ozonation reaction with the oxygen debit of 3 and 5 L/min at the third stage output voltage of 7.047 V_{dc} that could be calculated to determine the amount of residual ozone concentration has been produced. Table shows that each increment of time, it showed the increase in absorbing values.

Figure 16 shows the relationship between the concentration of ozone and the ozonation time in the setting of oxygen flow rate of 3 and 5 L/min from the battery source. These curves show the first, second and third stages of voltage. The concentration of ozone product due to the oxygen flow rate of 5 L/min would be higher than that 3 L/min. Besides that, the concentration of ozone product would rise as the voltage and the time

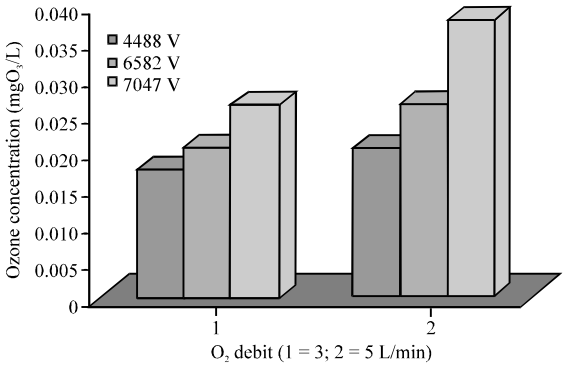

Fig. 17: The relationship between the remaining ozone concentration and and voltage levels for both 3 and 5 L/min of oxygen debits in the minute of 50 from the battery source

increased. The most substantial ozone formed was shown in the stage of 3 with the voltage of 7,047 V_{dc}, the oxygen flow rate of 5 L/min that produce ozone of 0.0382 mg O_3/L at 50 min.

Figure 17 shows the graph of residual ozone concentration to the voltage for 50 min. It can be seen that the formed ozone would increase as the voltage rise. It also reveals that the oxygen flow of 5 L/min would produced the ozone concentration greater than those the oxygen flow of 3 L/min from the battery source.

Based on the above figures and tables, it indicated that the most substantial ozone formed was shown in stage 3 with the voltage of 7.047 V_{dc} that produced ozone of 0.0382 mgO_3/L at 50 min. The corona could be seen without the use of visual aids by way of dimming the lights, so that the light emitted by the corona could be seen out through the tip end of the conductor. A corona was occurred if an electric field in the area around a conductor is higher than the field strength of air breakdown. The coronas due to electric field were occurred at both raised voltage of the battery and photovoltaic sources. The electric field magnitudes at the raised battery voltage source were greater than the photovoltaic source.

In the experiment using the direct source of solar panel, the ozone was produced by the three stages of generated voltage and by varying the flow rates of the oxygen debit of 3 and 5 L/min was with each experiment of 50 min and the recording data were in every 10 min. From the results of absorbing measurements to determine the concentration of residual generated ozone from each voltage using the calculation method of ozone concentration, it could be seen that the first stage of voltage produced 3.391 V_{dc} and the ozone product conducted by the rate of flow of oxygen debit of 5 L/min

was more than that debit of 3 L/min that was equal to 0.0118 mgO_3/L at minute of 50. In the second stage of voltage, it could be generated 6.250 V_{dc} and the ozone product conducted by varying the rate of flow of oxygen debit of 5 L/min was more than that debit of 3 L/min that was equal to 0.0206 mgO_3/L at 50 min. Finally, the third stage of generated voltage was 6.948 V_{dc} and the ozone product conducted by variation the flow rate of oxygen debit of 5 L/min was more than that the debit of 3 L/min that was as equal to 0.0323 mgO_3/L at 50 min.

In the experiments by using the source of battery, the generated ozone was produced by the 3 stages voltage levels, varying the flow rate of the oxygen debit of 3 and 5 L/min with each experiment 50 min and recording data per 10 min. The results of absorbing measurements to determine the concentration of generated residual ozone from each voltage level used the calculation method of ozone concentration, so that, it could be seen that the first stage was produced the voltage of 4.488 V_{dc} and the ozone results conducted by varying the rate of flow of oxygen to the debit of 5 L/min generated more ozone than the debit of 3 L/min was equal to 0.0206 mgO_3/L at 50 min. The second stage generated voltage of 6.582 V_{dc} and the ozone results conducted by varying the rate of oxygen flow to the debit of 5 L/min generated more ozone than the debit of 3 L/min that was equal to 0.0265 mgO_3/L at 50 min and the third stage voltage generated 7.047 V_{dc} and the ozone results were done with the flow rate variation oxygen debit of 5 L/min generated more ozone than the debit of 3 L/min that was equal to 0.0382 mgO_3/L at 50 min.

By doing two variations of the source of the above experiments, it could be seen that the source using the battery was better and produced more ozone due to the voltage on the battery was more stable. In contrast to the direct source of solar panel, although, the source voltage, 18 V_{dc}, greater than that the battery voltage, 12 V_{dc}, the output voltage after raising voltage using flyback circuit was smaller than the output voltage generated by the battery source. This case was predictly caused by the voltage on the photovoltaic was less stable, influenced by solar radiation and photovoltaic capacity. The discharge current generated by the solar panels was smaller than the current generated by the battery. The capacity of photovoltaic source was suspected as cause of smaller discharge current. Nevertheless, the voltage magnitude generated by the solar cell could be maintained in stable condition when using the battery and control charging with the constant voltage of 12 V_{dc}.

CONCLUSION

From the 18 V_{dc} source of the photovoltaic source at first stage, it was generated the high voltage of 3.391 V_{dc} and the ozone result conducted by the varying the flow rate of oxygen debit of 5 L/min generated more than that debit of 3 L/min that was equal to 0.0118 mgO_3/L at 50 min. From the 18 V_{dc} source of the photovoltaic panel at second stage, it was generated the high voltage of 6.250 V_{dc} and the ozone result conducted by the varying the flow rate of oxygen debit of 5L/min generated more than that debit of 3L/min that was equal to 0.0206 mgO_3/L at 50 min. From the 18 V_{dc} source of the photovoltaic at third stage, it was generated the high voltage of 6.948 V_{dc} and the ozone result conducted by the varying the flow rate of oxygen debit of 5 L/min generated more than that debit of 3 L/min that was equal to 0.0323 mgO_3/L at 50 min.

From the 12 V_{dc} source of the battery at first stage, it was generated the high voltage of 4.488 V_{dc} and the ozone result conducted by the varying the flow rate of oxygen debit of 5 L/min generated more than that debit of 3 L/min that was equal to 0.0206 mgO_3/L at 50 min. From the 12 V_{dc} source of the battery at second stage, it was generated the high voltage of 6.582 V_{dc} and the ozone result conducted by the varying the flow rate of oxygen debit of 5 L/min generated more than that debit of 3 L/min that was equal to 0.0265 mgO_3/L at 50 min. From the 12 V_{dc} source of the battery at third stage, it was generated the high voltage of 7.047 V_{dc} and the ozone result conducted by the varying the flow rate of oxygen debit of 5 L/min generated was more than that debit of 3 L/min that was equal to 0.0382 mgO_3/L at 50 min. The largest ozone result in oxygen debit of 3 L/min was produced by the third stage voltage at 0.0265 mgO_3/L whereas the largest ozone result of oxygen debit 5 L/min was generated by the third stage voltage of 0.0382 mgO_3/L.

The voltage source using battery was more stable and produced more ozone than that the photovoltaic panel. In contrast to the direct source of solar power, although, the source voltage was greater than the source voltage of the battery, however, after raising voltage using flyback circuit, it was smaller than the output voltage generated by the battery source. This case was predictly caused by the voltage on the photovoltaic energy source was not stable and influenced by solar radiation. The current generated by the photovoltaic panel was also smaller than that by the battery.

ACKNOWLEDGEMENT

This research was supported by the research institutions and community service (LP2M), Institut Teknologi Nasional Bandung (ITENAS).

REFERENCES

Amjad, M., Z. Salam, M. Facta and K. Ishaque, 2012. Design and development of a high-voltage transformer-less power supply for ozone generators based on a voltage-fed full bridge resonant inverter. J. Power Electron., 12: 387-398.

Amjad, M., Z. Salam, M. Facta and S. Mekhilef, 2013. Analysis and implementation of transformerless LCL resonant power supply for ozone generation. IEEE. Trans. Power Electron., 28: 650-660.

Anonymous, 2016. International trade administration, renewable energy market assessment report. United States Department of Commerce, Washington, DC., USA.

Boonseng, C., V. Kinnares and P. Apriratikul, 2000. Harmonic analysis of corona discharge ozone generator using brush electrode configuration. Proceedings of the IEEE International Conference on Power Engineering Society Winter Meeting Vol. 1, January 23-27, 2000, IEEE, Singapore, pp: 403-408.

Castle, G.P., I.I. Inculet and K.I. Burgess, 1969. Ozone generation in positive corona electrostatic precipitators. IEEE. Trans. Ind. General Appl., 4: 489-496.

Chalmers, I.D., L. Zanella and S.J. MacGregor, 1996. Ozone generation using pulsed corona in a wire/cylinder arrangement. Proceedings of the IEE International Conference on Colloquium on Pulsed Power, March 13, 1996, IEE, London, England, UK., pp: 1-7.

Charlangsut, A., M. Boonthienthong, S. Thongkeaw and P. Boonchiam, 2010. Study of ozone generator with electric fields distribution on water surfaces. Proceedings of the 2nd RMUTP International Conference on Green Technology and Productivity, June 29-30, 2008, Pathumwan, Princess Hotel, Bangkok, Thailand, pp: 1-4.

Fukawa, F., N. Shimomura, T. Yano, S. Yamanaka and K. Teranishi *et al*., 2008. Application of nanosecond pulsed power to ozone production by streamer corona. IEEE. Trans. Plasma Sci., 36: 2592-2597.

Goldman, M., A. Goldman and R.S. Sigmond, 1985. The corona discharge, its properties and specific uses. Pure Appl. Chem., 57: 1353-1362.

Hothongkham, P. and V. Kinnares, 2009. Analysis and modelling of an ozone generator using a phase-shift PWM full bridge inverter. Proceedings of the IEEE International Conference on Robotics and Biomimetics ROBIO, February 22-25, 2009, IEEE, Bangkok, Thailand, ISBN:978-1-4244-2678-2, pp: 1619-1624.

Izeki, N., 1983. Ozone generation mechanisms in ozonizer and future topics. Proc. Inst. Electrostat. Japan, 7: 142-149.

Jones, B., 1972. New Approaches to the Design and Economics of EHV Transmission Plant. Pergamon Press, Oxford, England, UK., Pages: 248.

Ketkaew, S., 2007. The case study of 5 kHz 25 kHz high frequency adjustment in converter circuit to generate ozone gas. Au. J. Tech., 11: 42-47.

LLC., 2015. Installation and owner's manual, corona discharge CD10/AD ozone generator. Limited Liability Company, Indian Harbour Beach, Florida.

Loeb, L.B., 1965. Electrical Coronas, their Basic Physical Mechanisms. University of California Press, Berkeley, California, USA., Pages: 695.

Lukes, P., M. Clupek, V. Babicky, V. Janda and P. Sunka, 2005. Generation of ozone by pulsed corona discharge over water surface in hybrid gas liquid electrical discharge reactor. J. Phys. D. Appl. Phys., 38: 409-416.

Ma, B., J. Andersson and S.M. Gubanski, 2010. Evaluating resistance of polymeric materials for outdoor applications to corona and ozone. IEEE. Trans. Dielectr. Electr. Insul., 17: 555-565.

Ma, B., S.M. Gubanski and H. Hillborg, 2011. AC and DC zone-induced ageing of HTV silicone rubber. IEEE. Trans. Dielectr. Electr. Insul., 18: 1984-1994.

Mattson, B., J. Michels, S. Gallegos, J. Ibanez and A. Alatorre-Ordaz, *et al*., 2007. Microscale gas chemistry, Part 28. Mini-Ozone generator: 800 nanomole/minute. Chem. News, 344: 6-11.

Mizuno, A., 2000. Electrostatic precipitation. IEEE. Trans. Dielectr. Electr. Insul., 7: 615-624.

Moon, J.D. and J.S. Jung, 2007. Effective corona discharge and ozone generation from a wire-plate discharge system with a slit dielectric barrier. J. Electrostat., 65: 660-666.

Moon, J.D., 1992. High efficiency ozone generation using a pyramidally embossed rod-to-cylinder electrode and a pulse corona discharge. Proc. Inst. Electrostat. Japan, 16: 224-229.

Nurendi, D.M., W. Waluyo and S. Syahrial, 2015. [Design and realization of corona generator with DC source from 12 volt DC battery using flyback converter (In Indonesia)]. Reka Elkomika, 3: 87-96.

Ohkubo, T., S. Hamasaki, Y. Nomoto, J.S. Chang and T. Adachi, 1990. The effect of corona wire heating on the downstream ozone concentration profiles in an air-cleaning wire-duct electrostatic precipitator. IEEE. Trans. Ind. Appl., 26: 542-549.

Panicker, P.K., F.K. Lu, G. Emanuel and B.T. Svihel, 2003. Ionization of air by corona discharge. Master Thesis, University of Texas at Arlington, Arlington, Texas.

Park, S.L., J.D. Moon, S.H. Lee and S.Y. Shin, 2006. Effective ozone generation utilizing a meshed-plate electrode in a dielectric-barrier discharge type ozone generator. J. Electrostat., 64: 275-282.

Patil, J.G. and T. Vijayan, 2010. Characteristics of high-tension-induced corona-discharge plasma in ozone generator diode. IEEE. Trans. Plasma Sci., 38: 2422-2427.

Pontiga, F., C. Soria, A. Castellanos and J.D. Skalny, 2001. Physicochemical modeling of ozone generation in a negative corona discharge. Proceedings of the International Conference on Electrical Insulation and Dielectric Phenomena, October 14-17, 2001, IEEE, Kitchener, Ontario, Canada, pp: 412-415.

Pontiga, F., H. Moreno and A. Castellanos, 2007. Ozone and Nitrogen oxides production by DC and pulsed corona discharge. Proceedings of the 2007 International Conference on Annual Report Electrical Insulation and Dielectric Phenomena (CEIDP), October 14-17, 2007, IEEE, Vancouver, British Columbia, ISBN:978-1-4244-1481-9, pp: 671-674.

Potivejkul, S., V. Kinnares and P. Rattanavichien, 1998. Design of ozone generator using solar energy. Proceedings of the 1998 IEEE International Conference on Asia-Pacific Circuits and Systems, November 24-27, 1998, IEEE, Chiangmai, Thailand, pp: 217-220.

Pressman, S., 2001. The story of Ozone. Plasmafire. Intl. Canada, 1: 1-58.

Samaranayake, W.J.M., E. Namihira, S. Katsuki, Y. Miyahara and T. Sakugawa *et al*., 2001. Pulsed power production of ozone using nonthermal gas discharges. IEEE. Electr. Insul. Mag., 17: 17-25.

Sathalalai, S. and W. Khan-ngern, 2012. The study of temperature effect in electrode rods for ozone generation. Eng. Appl. Sci. Res., 36: 323-331.

Schiavon, G.J., C.M.G. Andrade, L.M.L. Jorge and P.R. Paraiso, 2012. Design and analysis of ozone generator operating at high frequency with digital signal controller. Sci. Technol. Mag., 15: 23-35.

Seinfeld, J.H. and S.N. Pandis, 1998. Atmospheric Chemistry and Phyisics: From Air Pollution to Climate Change. John & Sons, Hoboken, New Jersey, USA., ISBN:9780471178163, Pages: 1326.

Simek, M. and M. Clupek, 2002. Efficiency of ozone production by pulsed positive corona discharge in synthetic air. J. Phys. D. Appl. Phys., 35: 1171-1175.

Smith, W., 2016. Principles of ozone generation. Watertec Engineering PTY Ltd., Beenleigh, Queensland.

Szczepanski, M., D. Malec, P. Maussion, B. Petitgas and P. Manfe, 2017. Ozone concentration impact on the lifespan of enameled wires (conventional and corona-resistant) for low voltage rotating machines fed by inverters. Proceedings of the 2017 IEEE International Conference on Electrical Insulation (EIC'17), June 11-14, 2017, IEEE, Baltimore, Maryland, ISBN:978-1-5090-3965-4, pp: 443-446.

Tsai, M.T. and C.W. Ke, 2009. Design and implementation of a high-voltage high-frequency pulse power generation system for plasma applications. Proceedings of the International Conference on Power Electronics and Drive Systems (PEDS'09), November 2-5, 2009, IEEE, Taipei, Taiwan, ISBN:978-1-4244-4166-2, pp: 1556-1560.

Tudoran, C.D., 2011. High frequency portable plasma generator unit for surface treatment experiments. Rom. J. Phys., 56: 103-108.

Udhayakumar, G., M.R. Rashmi, K. Patel, G.P. Ramesh and A. Suresh, 2016. Implementation of high-frequency high-voltage power supply for ozone generator system using embedded controller. Proceedings of the 2016 International Conference on Circuit, Power and Computing Technologies (ICCPCT'16), March 18-19, 2016, IEEE, Nagercoil, India, ISBN: 978-1-5090-1277-0, pp: 1-6.

Vijayan, T. and J.G. Patil, 2011. Temporal development of ozone generation in electron-induced corona-discharge plasma. IEEE. Trans. Plasma Sci., 39: 3168-3172.

Wojtowicz, J.A., 2001. Use of ozone in the treatment of swimming pools and spas. J. Swimming Pool Spa Ind., 4: 41-53.

Yanallah, K., F. Pontiga, A. Fernandez-Rueda, A. Castellanos and A. Belasri, 2008. Ozone generation using negative wire-to-cylinder corona discharge: The influence of anode composition and radius. Proceedings of the International Conference on Annual Report Electrical Insulation and Dielectric Phenomena (CEIDP), October 26-29, 2008, IEEE, Quebec, Canada, ISBN:978-1-4244-2548-8, pp: 607-610.

Yong-Nong, C. and K. Chih-Ming, 2013. Design of plasma generator driven by high-frequency high-voltage power supply. J. Appl. Res. Technol., 11: 225-234.